

ORIGINAL RESEARCH PAPER

The photo degradation of methyl red in aqueous solutions by $\alpha\text{-Fe}_2\text{O}_3/\text{SiO}_2$ nano photocatalyst

Majid Saghi^{*1}, Aref Shokri¹, Ali Arastehnodeh², Mohammad Khazaeinejad³, Atena Nozari⁴

¹ Young Researchers and Elite Club, Arak Branch, Islamic Azad University, Arak, Iran

² Department of Chemical Engineering, Quchan Branch, Islamic Azad University, Quchan, Iran

³ Department of Chemistry, Mashhad Branch, Islamic Azad University, Mashhad, Iran

⁴ Young Researchers and Elite Club, Quchan Branch, Islamic Azad University, Quchan, Iran

Received: 2018-04-17

Accepted: 2018-06-13

Published: 2018-08-10

ABSTRACT

The Photocatalytic degradation of chemical pollutants such as dyes, especially by Nano catalysts is an effective method to protect the environment and water resources. In this study, through Forced Hydrolysis and Reflux Condensation (FHRC) method the nanospherical $\alpha\text{-Fe}_2\text{O}_3$ particles were synthesized and supported on the surface of silica sand by Solid-State Dispersion (SSD) method with the average crystallite size of 27.5 nm. The characterization of catalyst and catalyst support was done using FTIR spectroscopy, SEM images, XRD patterns and BET surface area. In this paper, $\alpha\text{-Fe}_2\text{O}_3/\text{SiO}_2$ nano photocatalyst was used for the removal of methyl red (MR) under ultraviolet (UV) light. After running different tests, the effective parameters such as the concentration of MR, pH, and mass of catalyst on pollutant degradation were optimized by single-variable method. The results showed that the optimum conditions for achieving 98.46 % of degradation were pH at 5, initial concentration of MR at 10 mg/l, and 2.0 g of $\alpha\text{-Fe}_2\text{O}_3/\text{SiO}_2$ nano photo catalyst.

Keywords: Methyl Red, Nanophotocatalyst, Solid-State Dispersion (SSD) Method, $\alpha\text{-Fe}_2\text{O}_3/\text{SiO}_2$
© 2018 Published by Journal of Nanoanalysis.

How to cite this article

Saghi M, Shokri A, Arastehnodeh A, Khazaeinejad M, Nozari A. The photo degradation of methyl red in aqueous solutions by $\alpha\text{-Fe}_2\text{O}_3/\text{SiO}_2$ nano photocatalyst. J. Nanoanalysis., 2018; 5(3): 163-170. DOI: 10.22034/jna.2018.542765

INTRODUCTION

The penetration probability of different chemical pollutants to the water resources and finally environmental cycle always has been the main concern of environmental experts. Some of these pollutants because of their consistent molecular structure may remain constant many years in the environment and left their destructive effects on various creatures including human being [1]. Elimination of these chemical pollutants is not an easy work and needs using different new and effective methods [2]. The organic dyes are one of the most important categories of chemical pollutants with almost large molecular structures that easily penetrate environments, especially water resources and their elimination needs using advanced

methods. The MR considered as the most widely used organic dyes in different industries especially textile dyeing and paper printing industries [3]. This red dye is harmful and causing irritation in skin, eye and digestive tract if inhaled or swallowed. MR is a mitotic poison, mutagen and a suspected carcinogen [4-5].

Many different chemical and physical methods like chemical degradation (oxidation and molecular fractures) and or adsorption have been used for the elimination of MR up to this time [6-7]. Among chemical methods, complex of advanced oxidation processes (AOPs) is one of the most important, effective and high applied methods for the elimination of chemical pollutants [8-9]. Photocatalytic methods are part of AOPs in which

* Corresponding Author Email: m-saghi@iau-arak.ac.ir

one or some semiconductor catalysts activated or its activation increased through absorbing the energy of light. Through impacting the light to the catalyst, the huge amount of free radicals like hydroxyl radicals (OH^\bullet) was produced. The hydroxyl radicals can attack the pollutant molecules and convert them to mineral species such as H_2O and CO_2 [10]. ZnO , SiO_2 , Fe^{2+} , and Ag^+ doped TiO_2 are examples of the photocatalysts that used for degradation of pollutants [11-13]. In this regard, Iron oxide can also be used.

Hematite ($\alpha\text{-Fe}_2\text{O}_3$) with rhombohedral structure is the most common system of iron oxide that because of its various applications in several fields like magnetic materials, gas sensors, data storages, pigments and catalyst, has drawn attention of researchers and industries in recent years [14]. One of the most important applications of hematite is its application as a functional and effective support for environmental catalyst [15]. Studies show that hematite particles display more activity in nano scales, thus regarding their weight fewer amount would be needed to reach the desired goal.

So far, various techniques have been used for the synthesis of $\alpha\text{-Fe}_2\text{O}_3$ nanoparticles such as co-precipitation, sol-gel, sonochemical synthesis, Micelle synthesis, hydrothermal synthesis, thermal decomposition and FHRC methods [16-22].

Undoubtedly, the most important application of photocatalytic processes is water treatment; this claim is evident from the different published scientific reports in this field. The $\alpha\text{-Fe}_2\text{O}_3$ can be used as a fine powder or crystals dispersed in water, but after catalytic reaction, the filtering step is very difficult. In order to solve this problem, researchers have examined methods for supporting $\alpha\text{-Fe}_2\text{O}_3$ on the surface of organic, inorganic or organic-inorganic materials [23].

In the pollution removal process using the photocatalytic method, some materials with photocatalytic properties can be used as a catalyst support [24]. In such situations, catalyst support in addition to holding the catalyst helps to the degradation process. Different methods can be used in order to put the catalyst on the surface of the support. One of the easiest, high profits and the most cost-efficient methods is SSD in which catalyst precursor and catalyst support are mixed together with solid state. Then, the catalyst is formed during calcination and thermally positioned on the surface of catalyst support [25].

In this article, iron oxide nanoparticles are

synthesized through FHRC method and then thermally stabilized on the surface of silica sand by SSD technique. The prepared composite ($\alpha\text{-Fe}_2\text{O}_3/\text{SiO}_2$) used as a nanophotocatalyst for degradation and removal of MR in aqueous solution. For achieving the highest percentage of degradation, all the factors affecting the oxidation and degradation process were optimized through single variable method.

EXPERIMENTAL

Materials

All the chemicals used in this study were purchased from Merck Company and used without further purification. These materials included Iron (III) chloride hexahydrate, urea, MR, sulfuric acid 96%, sodium hydroxide and ethanol. Also, silica sand (particle size $< 0.04 \mu\text{m}$) was purchased from an Iranian company of Kimia Sadr (Yazd, Iran). Deionized water used in order for the solution preparation and washing the laboratory tools. The Molecular structure of MR is depicted in Fig. 1.

Apparatuses

The FTIR spectra, Surface morphology, BET surface area and X-ray diffraction patterns of silica and $\alpha\text{-Fe}_2\text{O}_3/\text{SiO}_2$ were performed using a Perkin-Elmer spectrophotometer (Spectrum Two, model), a Philips XL-30 SEM, a BELSORP-mini II BET instrument and a DX27-mini diffractometer, respectively. Also, all UV/Vis absorption spectra were obtained using an Agilent 8453 spectrophotometer.

Synthesis of $\alpha\text{-Fe}_2\text{O}_3$

According to Bharathi *et al.* [22], about 100 ml of urea 1 M was added to 100 ml iron (III) chloride 0.25 M slowly and drop by drop while stirring with magnetic stirrer. Then the resulting solution was placed under the reflux condition for 12 h at 90-95°C. The reflux sediment washed with deionized water to remove all unreactive materials. The washed sediment (iron hydroxide) was dried at

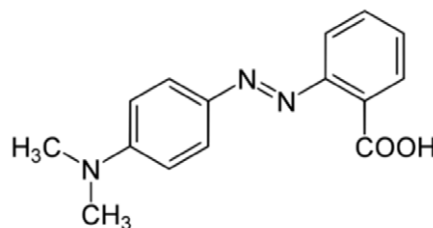


Fig. 1. Molecular structure of MR.

70°C and placed at 300°C for 1 h. The resulted solid with dark brown color was iron oxide.

Preparation of $\alpha\text{-Fe}_2\text{O}_3/\text{SiO}_2$ catalyst (SSD method)

According to Nikazar *et al.* [25], the produced iron hydroxide was mixed with SiO_2 in the proportion of 1:3 for preparation of $\alpha\text{-Fe}_2\text{O}_3/\text{SiO}_2$ catalyst using an agate pestle and mortar for 1 h. For easier mixing, a little quantity of ethanol was added to the mixture to obtain clay like state. After the full mixing process, the resulting mixture was dried and then it was positioned in the furnace for 1 h at 300 °C for calcination and conversion of supported iron hydroxide to iron oxide.

General procedure

The schematic of photocatalytic reactor used in this study showed in Fig. 2. The two mercury lamps, UV-C, 15 W from Philips Company of Holland were used as UV light sources and positioned on the upper section of the box. The radiation is generated almost exclusively at 254 nm. In order to perform any test, at first 1000 ml of MR contaminated water (with a definite concentration) was poured inside the reactor. The pH was adjusted by using NaOH and H_2SO_4 . A specific

quantity of catalyst was added to the reactor center while the lamps are turned on. The reaction time was calculated from the moment that catalyst was added and the lamps were illuminated. Sampling was done by a 5 ml syringe, every 20 min. In order to fully separate the catalyst from solution, the samples were centrifuged for 4 min with 3500 rpm speed. The concentration of MR solutions was determined at $\lambda_{\text{max}}=520$ nm. The photo degradation efficiency (x %) as a function of time is given as the following (Eq. 1) :

$$x\% = \frac{C_0 - C}{C_0} \times 100 \quad (1)$$

Where C_0 and C are the concentration of MR (mg/l) at $t=0$ and t, respectively. In the experiments, the initial concentration of MR varied from 10 to 50 mg/l (10, 20, 30, 40 and 50), pH varied from 3 to 11 (3, 5, 7, 9 and 11) and catalyst mass varied from 0.5 to 2.0 grams (0, 0.5, 1.0, 1.5 and 2.0 g) at five levels.

RESULT AND DISCUSSION

Characterization

The three different SEM images of catalyst support (silica) with various magnitudes ($\times 150$, $\times 850$ and $\times 46000$) were depicted in Fig. 3. Also,

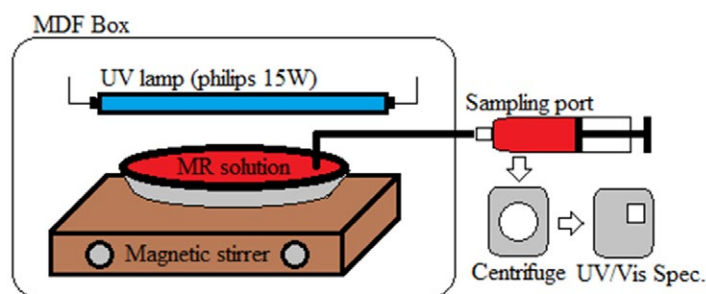


Fig. 2. Schematic diagram of photocatalytic reactor.

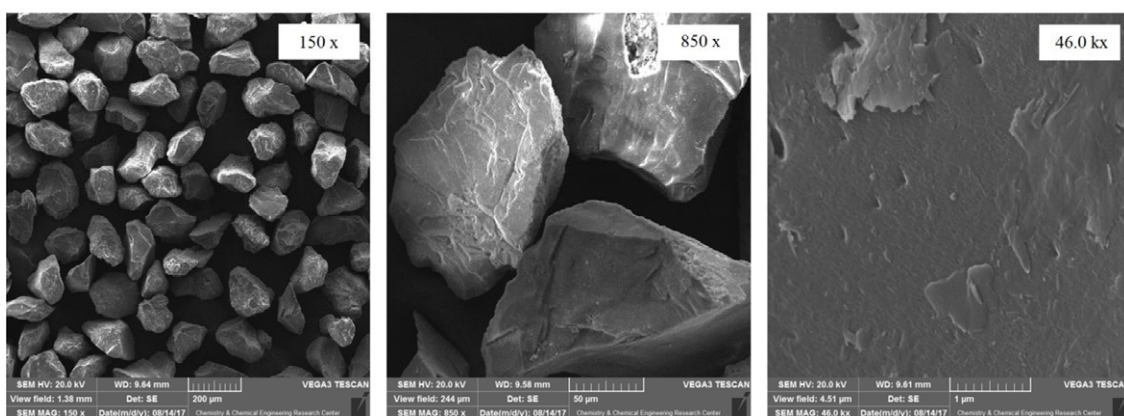


Fig. 3. The SEM images of silica (SiO_2).

three SEM images of $\alpha\text{-Fe}_2\text{O}_3/\text{SiO}_2$ catalyst with 850, 14000 and 46000 times magnification were presented in Fig. 4. At depicted images in Fig. 4, especially the middle one seems that particles of iron oxide spherically and uniformly dispersed on the surface of SiO_2 .

In Figs. 5a and 5b, the FTIR spectra of silica and $\alpha\text{-Fe}_2\text{O}_3/\text{SiO}_2$ have been shown, respectively. In spectrum 5a specific peak related to Fe-O vibration was labeled that because of the iron oxide existence in silica structure. The reason for the appearance of this peak is a natural existence of iron oxide in the mineral silica structure. This characteristic peak in 5b spectrum has more intensity that shows the

prosperous supporting of iron oxide on the surface of silica. Characteristic peaks of $\alpha\text{-Fe}_2\text{O}_3$ have well appeared and are in agreement with Bharati *et al.*, [22]. These characteristic peaks which are related to stretching and bending modes of OH and Fe-O binding in FeOOH , in some cases overlapped with absorption peaks of SiO_2 .

In Fig. 6, XRD patterns related to the SiO_2 (lower pattern) and $\alpha\text{-Fe}_2\text{O}_3/\text{SiO}_2$ (upper pattern) were depicted. As can be seen, characteristic peaks related to the SiO_2 in the lower pattern, without any changing in their position appear in the upper pattern. It shows that the structure of catalyst support (SiO_2) during the catalyst stabilization

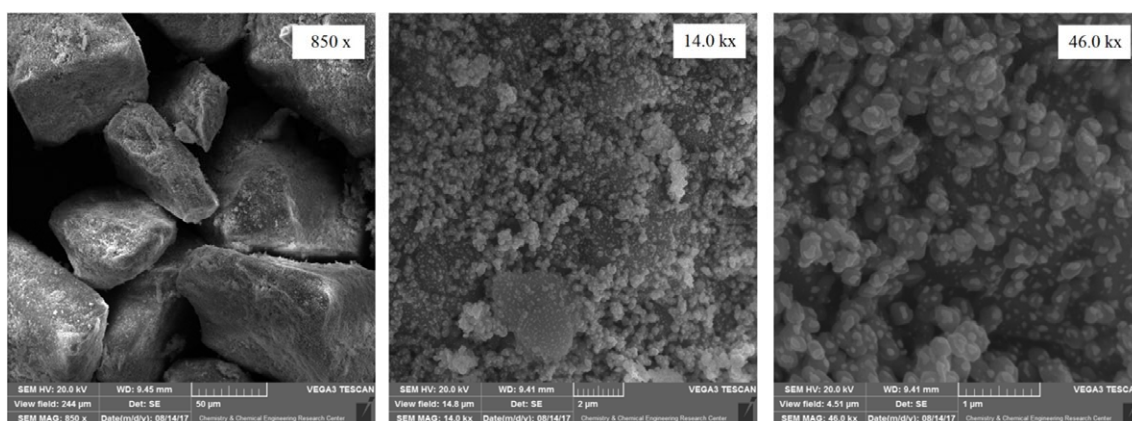


Fig. 4. SEM images of $\alpha\text{-Fe}_2\text{O}_3/\text{SiO}_2$ catalyst.

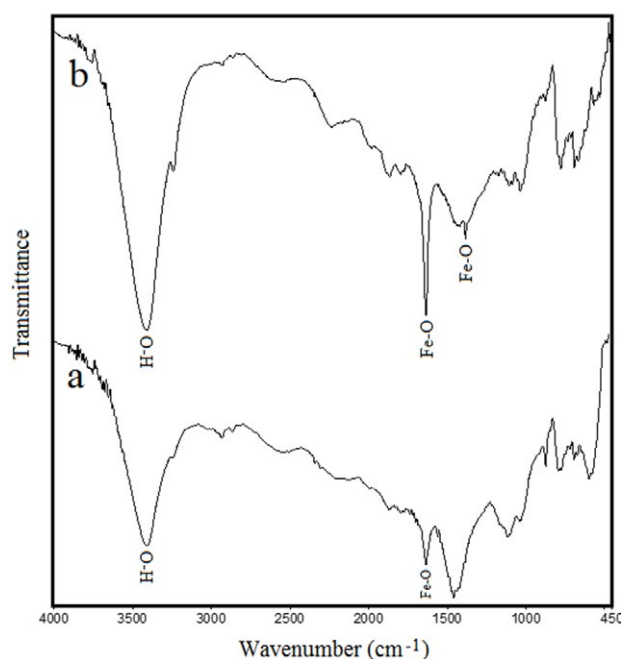


Fig. 5. FTIR spectra of Silica sand (a) and $\alpha\text{-Fe}_2\text{O}_3/\text{SiO}_2$ catalyst (b).

process was stable and did not change. In the upper pattern, $\alpha\text{-Fe}_2\text{O}_3$ -specified peaks (which also marked by vertical lines) appeared and it is in agreement with results of Bharati *et al.* [22]. Taking account of device errors, the crystallite size of spherical $\alpha\text{-Fe}_2\text{O}_3$ supported on the surface of silica was calculated by using XRD. The average crystallite sizes of the $\alpha\text{-Fe}_2\text{O}_3/\text{SiO}_2$ were calculated using the Debye-Scherrer Eq. (2) from the major diffraction peaks [15].

$$d = \frac{0.9\lambda}{\beta \cos\theta} \quad (2)$$

Where K is equal to 0.9 and β is the Perfect Width at Half- Maximum (FWHM) of the peak, λ is the wavelength of the used X-ray and θ is the Bragg angle. The average size of the crystalline was 27.5 nm for the $\alpha\text{-Fe}_2\text{O}_3$ based on SiO_2 . The nanoparticle size was obtained from the interpretation of XRD analysis but not from SEM images.

The surface area of materials was measured using BET device and N_2 adsorption-desorption method at 77 K. before the BET measurement, the materials were degassed under vacuum at 473 K for 12 h. The BET surface area of silica and $\alpha\text{-Fe}_2\text{O}_3/\text{SiO}_2$ were determined 18.33 and 61.45 (m^2/g), respectively. The BET results show that by supporting the iron oxide particles on the surface of silica, the catalyst surface area increased up to three times. It improves the catalyst performance because of increasing the

surface area, the number of available active sites for chemical reactions increased.

UV/Vis test of MR

The absorbance of MR solutions during photo degradation process at initial and after 20, 40, 60, 80, 100, 120, 140, 160 and 180 min of irradiation versus wavelength were shown in Fig. 7. Maximum wavelength (λ_{max}) in the absorption spectrum of MR was equal to 520 nm; Hence absorption of all samples after sampling read at $\lambda_{\text{max}} = 520$ nm.

Photocatalytic mechanism

When semiconductor catalyst absorbing energy, its electrons are transmitted from valence band (VB) to conduction band (CB). Indeed the initiation of photocatalytic process is through the giving energy to catalyst. When the UV light emitted on the supported $\alpha\text{-Fe}_2\text{O}_3$, the light's energy caused many electron-hole pairs in the catalyst. The VB potential (h_{VB}) is positive enough to generate hydroxyl radicals at the surface, and the CB potential (e_{CB}) is negative enough to reduce molecular oxygen. By generating the hydroxyl radicals, which are the strong oxidizing agent, the degradation of pollutants happens. The hydroxyl radicals attack to the molecular structure of pollutant on the surface or near the surface of catalysts and through its degradation gradually the contaminant eliminates [26].

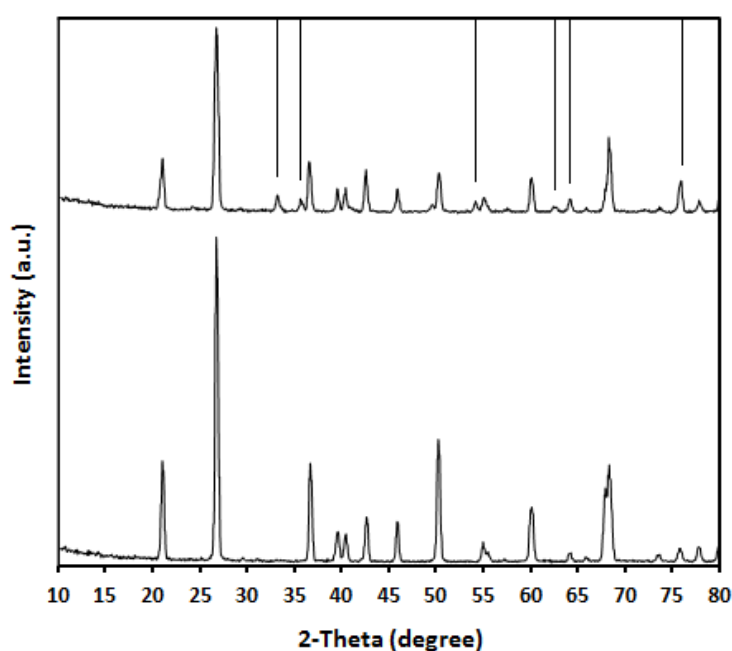


Fig. 6. X-ray diffraction of Silica sand (down) and $\alpha\text{-Fe}_2\text{O}_3/\text{SiO}_2$ catalyst (up).

According to this description, the photocatalytic degradation procedure of MR by UV light and $\alpha\text{-Fe}_2\text{O}_3/\text{SiO}_2$ catalyst can be written as the following (Eqs.3-12):

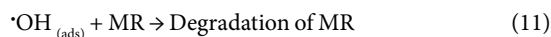
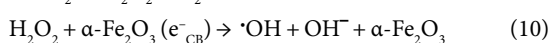
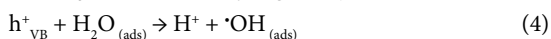
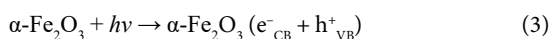


Fig. 8 shows a schematic diagram of the MR degradation process which represents the above mentioned reactions. A process continuously initiates by absorbing energy of light and terminate by degrading the molecular structure of MR using hydroxyl radicals and it converted to CO_2 and H_2O .

Effect of medium pH

The effect of pH on the removal percent of MR(X%) is presented in Fig. 9. As can be seen, the highest degradation percentage is obtained at pH=5. Regarding this diagram, generally, can be

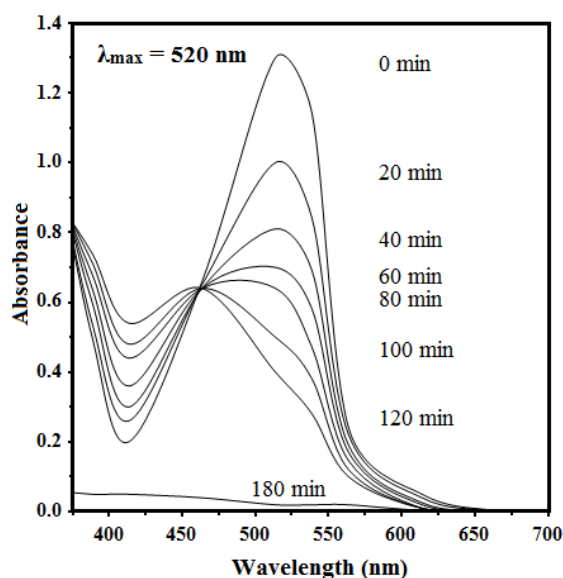


Fig. 7. UV/Vis spectral absorption changes of MR solution photodegraded by $\alpha\text{-Fe}_2\text{O}_3/\text{SiO}_2$.

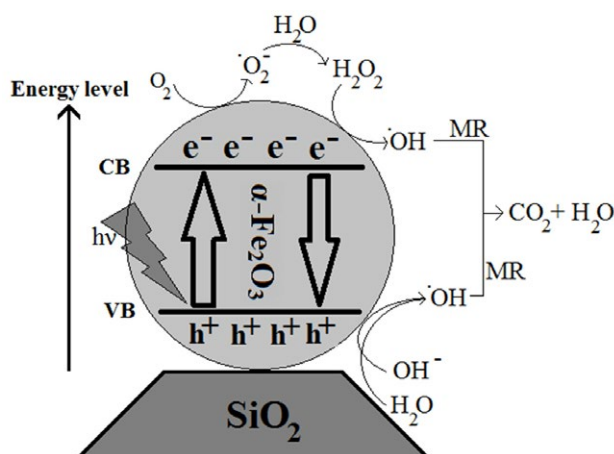


Fig. 8. Schematic diagram of photocatalytic reactions for MR degradation.

said that between pH=5-7 the highest degradation percentage is attained. The Point of zero charge (PZC) of the catalyst $\alpha\text{-Fe}_2\text{O}_3/\text{SiO}_2$ was tested and it was 5. At this pH, the surface charge of the catalyst was zero, above this pH the surface charge of the catalyst was negative and below this pH, the surface charge of the catalyst was positive.

Also, the results showed that at alkali mediums (pH>7) degradation amount sharply decreased. Because in alkali mediums the surface area of Fe_2O_3 particles negatively charged, attracts more positively charged specimens. On the other hand, MR is an anionic dye and attracted by Fe_2O_3 particles less in alkali mediums so its degradation was low. This is the reason that why degradation percentage decreased as pH increased. At pH values below than 5.3, MR dye has the cationic form [3]; on the other hand, in acidic medium surface of Fe_2O_3 particles is positively charged, for these reasons at pH of 5, the molecules of MR dye attracted by particles of catalyst and the x% partly increased. Decreasing of x% by reducing pH from 5 to 3 has happened because of leaching of $\alpha\text{-Fe}_2\text{O}_3$ from the support of catalyst. Therefore, at pH=5 the highest degradation amount (75.40 %) was obtained.

Effect of the initial Concentration of MR

The effect of initial concentration of MR on x% in optimum pH (pH=5) is shown in Fig. 10. As can be seen, the amount of degradation was decreased with increasing in the concentration of MR. By increasing the number of MR molecules in the reactor, catalyst and light need more time to degrade the MR fully, therefore by increasing the concentration of MR degradation amount was decreased. Also, the UV light can be made to go more easily through the solution to irradiate the catalyst when the initial concentration of MR is lower, hence, photocatalytic efficiency increased by decreasing the initial concentration of MR.

Effect of catalyst mass

Fig. 11 showed a diagram related to the effect of catalyst mass on x% under optimum conditions: pH=5 and initial concentration of MB=10 mg/l. Results showed that as the catalyst mass increased degradation of MR increased up to the point that by using 2 g of catalyst after 120 min of reaction, 98.46 % of MR eliminated. By devoting more attention to the diagram represented in Fig. 11, it could be seen that by using 0 g of catalyst, 7.86% of MR was removed. This amount of degradation occurred

because of the exposure of UV light to the solution and partial degradation of pollutant. By increasing the catalyst mass, the number of free electrons in CB was increased and these free electrons produce more free radicals. Therefore, increasing the mass of catalyst increases the x% [27].

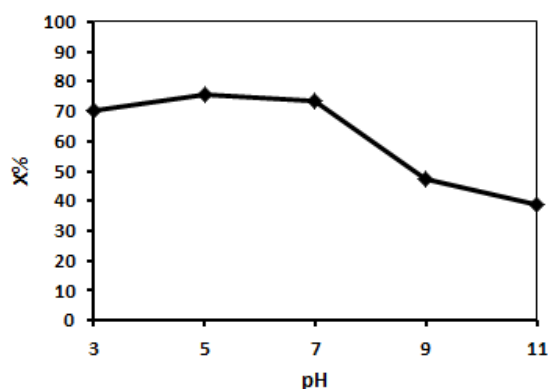


Fig. 9. The effect of pH on the removal percent of MR(X%) (initial concentration of MR at 30 mg/l, Catalyst mass at 1.0 g and reaction time in 120 min).

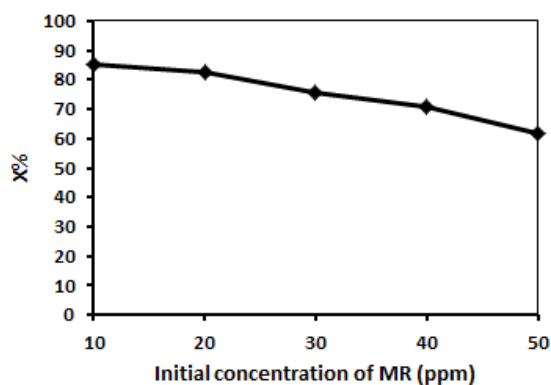


Fig. 10. The effect of initial concentration of MR on x% (pH=5, Catalyst Mass=1.0 g, reaction time=120 min).

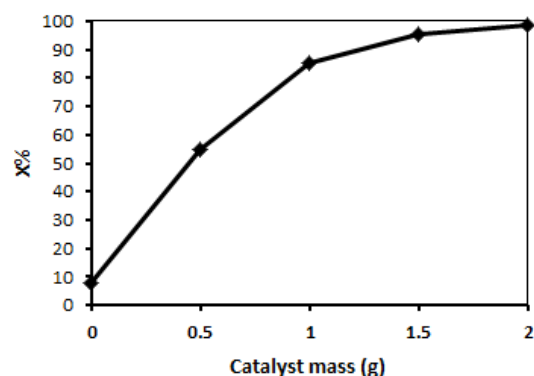


Fig. 11. The effect of the mass of $\alpha\text{-Fe}_2\text{O}_3/\text{SiO}_2$ catalyst on x% (pH=5, initial concentration of MR at 10 mg/l, reaction time at 120 min, volume of MR solution at one liter).

CONCLUSION

In this study iron hydroxide particles as catalyst precursor by FHRC method were prepared and used. The iron hydroxide was prepared by conventional and low-cost method of SSD and then supported on the surface of mineral silica at 300 °C. The average crystallite sizes of the $\alpha\text{-Fe}_2\text{O}_3/\text{SiO}_2$ were obtained at 27.5 nm through the XRD analysis and the Debye–Scherer equation. The properties of catalyst and its support was explored by FT-IR spectroscopy, SEM images, XRD patterns and BET surface area. The FT-IR technique shows that the structure of SiO_2 during inserting of $\alpha\text{-Fe}_2\text{O}_3$ on it was stable and did not change. The $\alpha\text{-Fe}_2\text{O}_3/\text{SiO}_2$ was employed as a nanophotocatalyst for degradation of MR dye. The efficient parameters on degradation such as pH, the initial concentration of MR and catalyst mass were optimized by single-variable method. Results showed that under the optimum conditions, including pH at 5, initial concentration of MR at 10 mg/l, and 2 g of catalyst, about 98.46% of MR were degraded after 120 min of reaction.

ACKNOWLEDGEMENT

The authors of this paper thanks and appreciate the Maghsoud porcelain group (Mashhad, IRAN) because of their material and spiritual supports.

CONFLICT OF INTEREST

The authors declare that there is no conflict of interests regarding the publication of this manuscript.

REFERENCES

1. A. Shokri, K. Mahanpoor and D. Soodbar, *Desalin. Water Treat.*, 57, 16473 (2016). <https://doi.org/10.1080/19443994.2015.1085454>
2. C. Fernandez, M.S. Larrechi and M.P. Callao, *TrAC, Trends Anal. Chem.*, 29, 1202 (2010). <http://www.sciencedirect.com/science/article/pii/S0165993610002190>
3. N.K. Singh, S. Saha and A. Pal, *Desalin. Water Treat.*, 56, 1066 (2015). <https://doi.org/10.1080/19443994.2014.942380>
4. P.P. Vijaya and S. Sandhya, *Environmentalist*, 23, 145 (2003). <https://doi.org/10.1023/A:1024839805387>
5. Y. Badr, M.G. Abd El-Wahed and M.A. Mahmoud, *J. Hazard. Mater.*, 154, 245 (2008). <https://doi.org/10.1016/j.jhazmat.2007.10.020>
6. A. Bhattacharya, N. Goyal and A. Gupta, *Extremophiles*, 21, 479 (2017). <https://dx.doi.org/10.1007/s00792-017-0918-2>
7. E.A. Khan, Shahjahan and T.A. Khan, *J. Mol. Liq.*, 249, 1195 (2018). <https://doi.org/10.1016/j.molliq.2017.11.125>
8. A. Galenda, L. Crociani, N. El Habra, M. Favaro, M.M. Natile and G. Rossetto, *Appl. Surf. Sci.*, 314, 919 (2014). <https://doi.org/10.1016/j.apsusc.2014.06.175>
9. A. Shokri, *Desalin. Water Treat.*, 58, 258 (2017). <https://doi.org/10.5004/dwt.2017.0292>
10. A. Shokri, K. Mahanpoor and D. Soodbar, *J. Environ. Chem. Eng.*, 4, 585 (2016). <https://doi.org/10.1016/j.jece.2015.11.007>
11. Aref Shokri, *Int. J. Nano Dimens.*, 7 (2), 160(2016). <https://doi.org/10.7508/ijnd.2016.02.008>
12. C. Sahoo, A.K. Gupta and A. Pal, *Desalination*, 181, 91 (2005). <https://doi.org/10.1016/j.desal.2005.02.014>
13. M. Mohaddasi, A. Shokri, *Desal. Water Treat.*, 81,199 (2017). <https://doi.org/10.5004/dwt.2017.21182>
14. M. Saghi and K. Mahanpoor, *Int. J. Ind. Chem.*, 8, 297 (2017). <https://doi.org/10.1007/s40090-016-0108-6>
15. A. Shokri, F. Rabiee and K. Mahanpoor, *Int. J. Environ. Sci. Technol.*, 14, 2485 (2017). <https://doi.org/10.1007/s13762-017-1346-7>
16. M. Farahmandjou and F. Soflaee, *Phys. Chem. Res.*, 3, 191 (2015). [10.22036/pcr.2015.9193](https://doi.org/10.22036/pcr.2015.9193)
17. H. Liang, K. Liu and Y. Ni, *Mater. Lett.*, 159, 218 (2015). <https://doi.org/10.1016/j.matlet.2015.06.103>
18. M. Diab and T. Mokari, *Inorg. Chem.*, 53, 2304 (2014). [10.1021/ic403027r](https://doi.org/10.1021/ic403027r)
19. T. Jiang, A.S. Poyraz, A. Iyer, Y. Zhang, Z. Luo, W. Zhong, R. Miao, A.M. El-Sawy, C.J. Guild, Y. Sun, D.A. Kriz and S.L. Suib, *J. Phys. Chem. C*, 119, 10454 (2015). [10.1021/acs.jpcc.5b02057](https://doi.org/10.1021/acs.jpcc.5b02057)
20. A. Askarinejad, M. Bagherzadeh and A. Morsali, *J. Exp. Nanosci.*, 6, 217 (2011). <https://doi.org/10.1080/17458080.2010.489583>
21. M. Tadic, M. Panjan, V. Damnjanovic and I. Milosevic, *Appl. Surf. Sci.*, 320, 183 (2014). <https://doi.org/10.1016/j.apsusc.2014.08.193>
22. S. Bharathi, D. Nataraj, D. Mangalaraj, Y. Masuda, K. Senthil and K. Yong, *J. Phys. D: Appl. Phys.*, 43, 1 (2010). [10.1088/0022-3727/43/1/015501](https://doi.org/10.1088/0022-3727/43/1/015501)
23. M. Chen, J. Liu, D. Chao, J. Wang, J. Yin, J. Lin, H.J. Fan and Z.X. Shen, *Nano Energy*, 9, 364 (2014). <https://doi.org/10.1016/j.nanoen.2014.08.011>
24. K. Zhao, Y. Lu, N. Lu, Y. Zhao, X. Yuan, H. Zhang, L. Teng and F. Li, *Appl. Surf. Sci.*, 285, 616 (2013). <https://doi.org/10.1016/j.apsusc.2013.08.101>
25. M. Nikazar, K. Gholivand and K. Mahanpoor, *Desalination*, 219, 293 (2008). <https://doi.org/10.1016/j.desal.2007.02.035>
26. A. Shokri, K. Mahanpoor, *Int J Ind Chem* 8,101, (2017). <https://doi.org/10.1007/s40090-016-0110-z>
27. A. Shokri, A. Hassani Joshagani, *Rus. J. appl. Chem.*, 89, 1985(2016). <https://doi.org/10.1134/S1070427216120090>